

# NAVAL POSTGRADUATE SCHOOL MONTEREY, CALIFORNIA



## THESIS

### BURIED OBJECT DETECTION USING SURFACE WAVES

by

William F. Stewart

September, 1995

Thesis Advisor:

Anthony A. Atchley

Approved for public release; distribution is unlimited.

19960327 069

DTIC QUALITY INSPECTED 1

REPORT DOCUMENTATION PAGE			Form Approved OMB No. 0704-0188	
Public reporting burden for this collection of information is estimated to average 1 hour per response, including the time for reviewing instruction, searching existing data sources, gathering and maintaining the data needed, and completing and reviewing the collection of information. Send comments regarding this burden estimate or any other aspect of this collection of information, including suggestions for reducing this burden, to Washington Headquarters Services, Directorate for Information Operations and Reports, 1215 Jefferson Davis Highway, Suite 1204, Arlington, VA 22202-4302, and to the Office of Management and Budget, Paperwork Reduction Project (0704-0188) Washington DC 20503.				
1. AGENCY USE ONLY (Leave blank)		2. REPORT DATE 10 September 1995		3. REPORT TYPE AND DATES COVERED Master's Thesis
4. TITLE AND SUBTITLE BURIED OBJECT DETECTION USING SURFACE WAVES			5. FUNDING NUMBERS	
6. AUTHOR(S) William F. Stewart				
7. PERFORMING ORGANIZATION NAME(S) AND ADDRESS(ES) Naval Postgraduate School Monterey CA 93943-5000			8. PERFORMING ORGANIZATION REPORT NUMBER	
9. SPONSORING/MONITORING AGENCY NAME(S) AND ADDRESS(ES)			10. SPONSORING/MONITORING AGENCY REPORT NUMBER	
11. SUPPLEMENTARY NOTES The views expressed in this thesis are those of the author and do not reflect the official policy or position of the Department of Defense or the U.S. Government.				
12a. DISTRIBUTION/AVAILABILITY STATEMENT Approved for public release; distribution is unlimited.			12b. DISTRIBUTION CODE	
13. ABSTRACT  The goal of this thesis is to evaluate the use of surface waves to detect buried objects. The source used to generate the surface waves was a three element phased array controlled by LabVIEW visual instruments. This research included developing a source and receiver, evaluating attenuation and azimuthal dependence of the surface wave propagation, detection using scattering within a tank of sand, and using the three element array to beamform surface waves. It was successfully demonstrated that target localization using surface wave scattering and beamforming with a phased array is possible.				
14. SUBJECT TERMS mine detection; Rayleigh waves; acoustic mine detection; surface waves			15. NUMBER OF PAGES 64	
			16. PRICE CODE	
17. SECURITY CLASSIFICATION OF REPORT Unclassified	18. SECURITY CLASSIFICATION OF THIS PAGE Unclassified	19. SECURITY CLASSIFICATION OF ABSTRACT Unclassified	20. LIMITATION OF ABSTRACT UL	

NSN 7540-01-280-5500

Standard Form 298 (Rev. 2-89)

Prescribed by ANSI Std. Z39-18 298-102



Approved for public release; distribution is unlimited

BURIED OBJECT DETECTION  
USING  
SURFACE WAVES

William F. Stewart  
Lieutenant, United States Navy  
B.S., University of Maryland, 1984

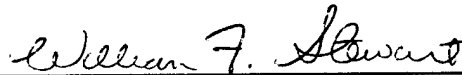
Submitted in partial fulfillment  
of the requirements for the degree of

**MASTER OF SCIENCE IN ENGINEERING ACOUSTICS**

from the

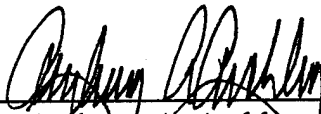
**NAVAL POSTGRADUATE SCHOOL**  
**September 1995**

Author:



William F. Stewart

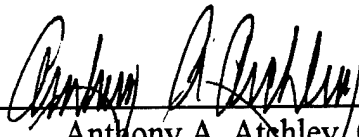
Approved by:



Anthony A. Atchley, Thesis Advisor



Clyde Scandrett, Co-Thesis Advisor



Anthony A. Atchley, Chairman  
Engineering Acoustics Academic Committee



## **ABSTRACT**

The goal of this thesis is to evaluate the use of surface waves to detect buried objects. The source used to generate the surface waves was a three element phased array controlled by LabVIEW visual instruments. This research included developing a source and receiver, evaluating attenuation and azimuthal dependence of the surface wave propagation, detection using scattering within a tank of sand, and using the three element array to beamform surface waves. It was successfully demonstrated that target localization using surface wave scattering and beamforming with a phased array is possible.



## TABLE OF CONTENTS

I. INTRODUCTION.....	1
A. OBJECTIVE.....	1
B. MOTIVATION.....	1
C. BACKGROUND.....	2
D. STEPS OF RESEARCH.....	4
II. DEVELOPMENT AND DESIGN.....	5
A. WAVE PROPAGATION IN SOLIDS.....	5
B. TEST TANK.....	7
C. THE SOURCE.....	8
D. THE RECEIVER.....	9
E. SUPPORTING EQUIPMENT.....	10
F. DATA AQUISITION SYSTEM.....	12
III. CHARACTERISTICS OF A POINT SOURCE.....	13
A. RADIAL DEPENDENCE.....	13
1. Procedure.....	13
B. AZIMUTHAL DEPENDENCE.....	16
1. Procedure.....	16
C. SCATTERING FROM A BURIED OBJECT.....	17
IV. PHASED ARRAY BEAMFORMING.....	29
A. BEAMFORMING.....	29
B. BEAMFORMING MODEL.....	29



C. EXPERIMENT.....	30
V. CONCLUSION.....	37
A. RESULTS.....	37
APPENDIX A. FACTSHEET FOR SOURCE ELEMENT.....	39
APPENDIX B. LABVIEW VI FOR INTENSITY FIELD STUDY.....	41
APPENDIX C. LABVIEW VI FOR DATA AQUISITION.....	43
APPENDIX D. MATLAB PROGRAM FOR ELLIPSE PLOTTING.....	45
APPENDIX E. MATLAB PROGRAM OF BEAMFORMING ARRAY.....	47
APPENDIX F. LABVIEW VI FOR BEAMFORMING ARRAY.....	49
LIST OF REFERENCES.....	51
INITIAL DISTRIBUTION LIST.....	53

## LIST OF FIGURES

1.1	Compressional wave and Rayleigh wave.....	6
1.2	Rayleigh wave propagation.....	6
1.3	Source design .....	8
1.4	Receiver ground coupling methods.....	9
1.5	Lab set-up.....	11
3.1	Attenuation in sand.....	14
3.2	Value of attenuation coefficients.....	15
3.3	Attenuation measurements by Chotiros.....	16
3.4	Front panel Intensity Field vi.....	19
3.5	Azimuthal dependence of waveform.....	20
3.6	Front panel Signal Averaging vi.....	21
3.7	Front panel Comparison vi.....	22
3.8	Elliptical points of reflected path.....	23
3.9	Comparison of 004 degree path.....	24
3.10	Comparison of 036.2 degree path.....	25
3.11	Comparison of 079 degree path.....	26
3.12	Plot of ellipitcal paths.....	27
4.1	Beamforming vi Front Panel.....	31
4.2	Received pulses at indicated bearings.....	32
4.3.	Calculated beam pattern for three element array.....	33
4.4	Signal with and without beamforming.....	35
A.1	Factsheet for source element.....	39

B.1	Elements of Intensity Field vi.....	41
B.2	Field intensity vi.....	42
C.1	Elements of Data Acquisition vi.....	44
C.2	Data Aquisition vi.....	44
F.1	Elements of Three Element Function Generator vi.....	49
F.2	Three Element Array Function Generator vi.....	50

## **I. INTRODUCTION**

### **A. OBJECTIVE**

The purpose of this research was to evaluate the feasibility of using a phased array to generate surface waves to detect buried land/sea mines.

### **B. MOTIVATION**

The detection of buried mines in the ocean bottom, surf zone and on land is a continuing civil and military problem. In October, 1994 the United Nations Secretary General Boutros Boutros-Ghali commented that the estimated number of mines still in place from conflicts of this century is over 100 million through within 62 countries [Ref 1]. These mines, originally intended to disrupt commercial activity, utility plant operations, port facilities, transportation routes, and troop movement take their toll on postwar civilian populations throughout the world. The technology to safely and efficiently remove land mines has not been developed. The current cost of removing a single \$25 anti-personnel mine is estimated by the United Nations [Ref 1] to ranges from \$300 - \$1000. This cost is projected to be higher as popular plastic mines render magnetic mine clearance devices currently in use obsolete.

The strategic advantage gained from the Iraqi mine field in the Persian Gulf can be debated, given the results of the war. However, there is no question that it was effective in damaging two US warships, altering the assault objective to Faylakah Island, and

preventing the amphibious assault on Kuwait. At the end of the Persian Gulf war 1,300 mines were recovered with 24% being bottom mines in various states of scouring according to the Center for Security Strategies and Operations [Ref 2]. These mines could have had a much greater impact on the outcome of the war and the number of personnel and material losses had a different assault plan been chosen. Set up as a barrier to amphibious assault, the Iraqi mine field was successfully avoided and removed once it was discovered. If the mines had been used more effectively to hamper the positioning of ships or if amphibious assault had been an only option, mine clearance would have been a much bigger problem than as it turned out.

As implied in “. . .From the Sea,” for our current naval doctrine to work, some method of rapid detection of mines must be developed to deal with buried mines.

### **C. BACKGROUND**

For more than 25 years the US. Navy has utilized marine mammals to detect objects in the water and buried in the ocean floor. The continuing study of these animals and how their sensor systems work could provide valuable insights for the next generation of sonar for mine detection. In a similar fashion, sand scorpions of the Mojave desert, who are able to capture their prey by detecting Rayleigh waves, might have some of the answers for buried mine detection, [Ref 3]. Utilizing their eight independent

tarsal slit sensilla as vibration receptors, scorpions are able to detect small vibrations in the sand resulting from the Rayleigh surface waves and compression waves (P waves) created by the movement of their prey. They are then able to accurately estimate time differences between arrivals of the two types of waves in order to formulate target distance and direction from the timing and ordering of signals received by their sensors. At distances of 10 cm they can derive target angle and distance very accurately and tests have shown they can detect disturbances out to 30 cm [Ref 3].

In elastic media, Rayleigh waves propagate with a non-dispersive speed slower than the shear and compression wave speeds of the medium. Because Rayleigh waves are localized to within a few wavelengths of the surface of the medium they could be ideal for hunting mines that must be placed near the surface to be effective. From 1987 to 1992, BBN Systems and Technology undertook a feasibility study to design an experimental system for detecting and locating buried land mines using acoustical probing [Ref 4]. In their report, BBN employed source and receiver arrays which achieved detection distances of 15 feet. The source used in that work was a water filled tube in which a high voltage electrode created a spark. The resulting pressure wave was transmitted through a rubber membrane in contact with the ground. It is estimated that only 67% of the energy from a point source energy is propagated in the form of Rayleigh waves. The remaining energy is disbursed in the form of downgoing vertically polarized shear (SV)

waves (23%) and compression (P) waves (10%). Coupled with no source directivity, BBN's system is inefficient as a method of generating surface waves.

The focus of the research presented in this thesis is to build an improved surface wave source. The source will consist of a phased array of several discrete sources, operated at an optimal frequency for the specific soil type.

#### **D. STEPS OF RESEARCH**

The stages of research involved:

1. Building an appropriate test tank.
2. Developing sources and receivers.
3. Develop data acquisition software using LabVIEW.
4. Measuring the performance of a three element array of sources.

## **II. DEVELOPMENT AND DESIGN**

The purpose of this chapter is to 1) review the characteristics of Rayleigh waves, 2) discuss the test tank, source and receiver used in this research, and 3) discuss the LabVIEW-based data acquisition system.

### **A. WAVE PROPAGATION IN SOLIDS**

A point source acting at the surface of an elastic medium excites three basic types of waves: compressional waves, shear waves, and surface waves. Compressional waves are characterized by particle motion along the direction of propagation, whereas in shear waves the motion is transverse to the direction of propagation. Both of these types of waves can exist within the bulk of the solid and spread spherically away from a point source. Surface waves, as the name implies, are confined to the surface of the medium [see Figure (1.1)]. Their amplitude decays exponentially with distance from the surface, with a decay constant approximately equal to the wavelength. As a result of their confinement to the surface, the propagation is cylindrical in nature. The particle motion is a retrograde ellipse, confined to the vertical plane, Figure (1.2). The speed of propagation is less than the shear wave speed for the medium. Surface waves are commonly referred to as Rayleigh waves, although strictly speaking, Rayleigh wave is the correct name only for the case of a wave on the surface bounding



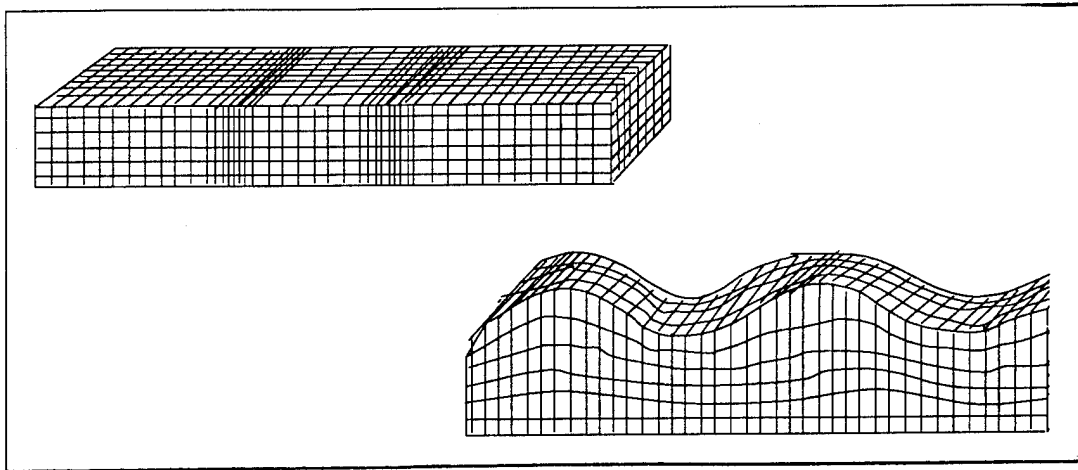


Figure (1.1) Compressional wave and Rayleigh wave.

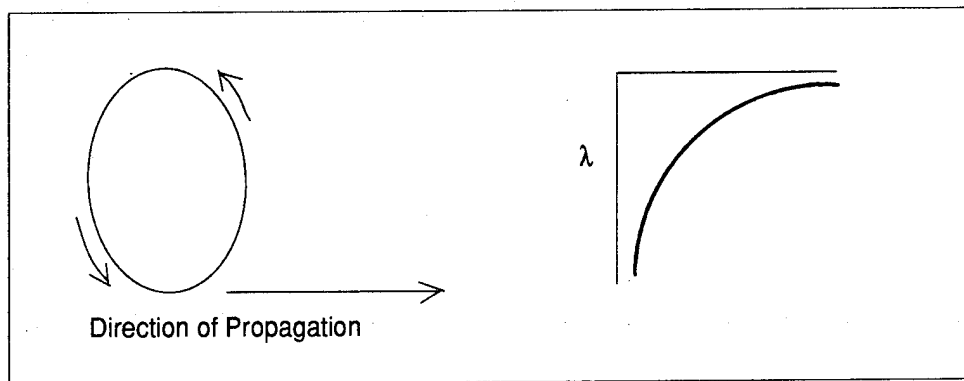


Figure (1.2). Rayleigh wave propagation.

a semi-infinite elastic medium and vacuum. However, for practical purposes the physics of Rayleigh waves accurately describes the practical situation of a wave on the surface of a solid, many surface-wavelengths thick, with air above.

## **B. TEST TANK**

In this thesis we want to investigate the propagation of surface waves at an air/wet sand interface in a controlled, laboratory environment. The first step is to establish a suitable environment. Preliminary tests were performed in a 1.1 m x 3 m, fiberglass lined wooden tank, filled with approximately 60 cm of wet sand. The purpose of these preliminary measurements were to determine approximate surface wave speeds, and therefore wavelengths. The results indicated wave speeds in the range 60 - 90 m/s. The corresponding wavelengths for frequencies from 300 - 2000 Hz are approximately 25 - 4 cm. Therefore, we need a sand depth of approximately 1 m to mimic a semi-infinite medium at the lowest frequencies of interest. The width of the tank needed to be as large as possible to prevent interference with reflections from its sides. These conditions were approximately met by a twelve foot diameter, four foot deep redwood tank. This tank was filled with approximately 17 tons of medium gain (.6 mm) beach sand from Moss Landing in Monterey County, California. The sand was washed to remove salt and filtered for large objects. Using a garden hose with spray attachment the surface was uniformly wetted prior to each experiment.

## **C. THE SOURCE**

The source design was guided by the following requirements:

1. It should be a vertical point source that could generate

signals with sufficient amplitude to allow detection of surface waves anywhere in the test tank.

2. It should provide a repeatable waveform.
3. It should be capable of high repetition rates.
4. It should have good ground coupling that would last for an extended period.
5. It should provide clean signals over a range of frequencies, from approximately 300-2000 Hz.

In addition, it had to be relatively inexpensive and easily modified given the time and resources available. It was therefore not the intent of this research to develop a working unit for mass production. After various types of drivers were tested it was found that a four inch diameter, high cone excursion, electrodynamic speaker with an aluminum 45 degree angle cone attached to the center of the diaphragm, worked well. In addition, a 25 gram mass was added to the cone appendage to improve ground coupling. (Figure(1.3), factsheet Appendix (A).

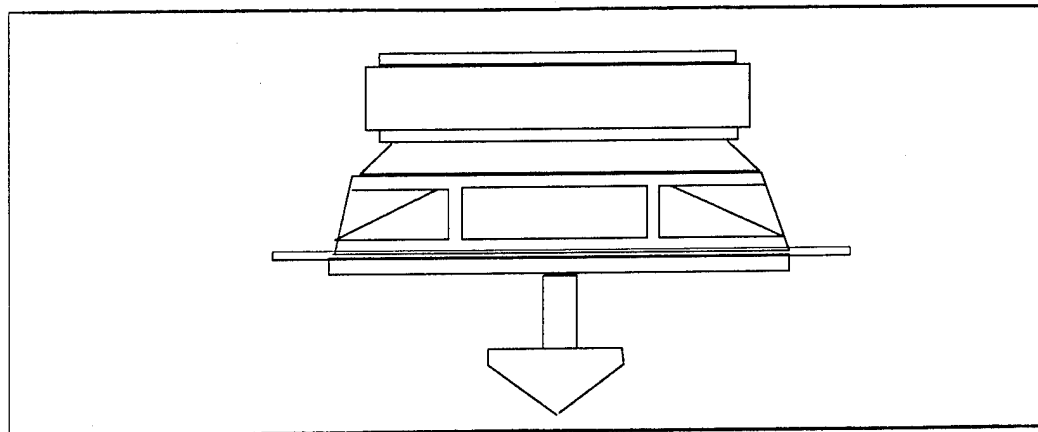


Figure (1.3) Source design.

#### D. THE RECEIVER

The design requirements for a receiver to detect ground vibration for this research were to provide:

1. Adequate sensitivity to ground motion generated by the source within the distances of the tank.
2. Broadband response.
3. Good ground coupling that could give repeatable results.

Several different designs were tried. The initial design focused on using a piezo-electric disk. The disks were acquired from small audio speakers available from any commercial electronics shop. The disks had appendages glued to them to provide coupling to the ground. They also had a mass attached with the top to improve coupling and reduce ringing. Figure (1.4) shows the different appendages that were tried.

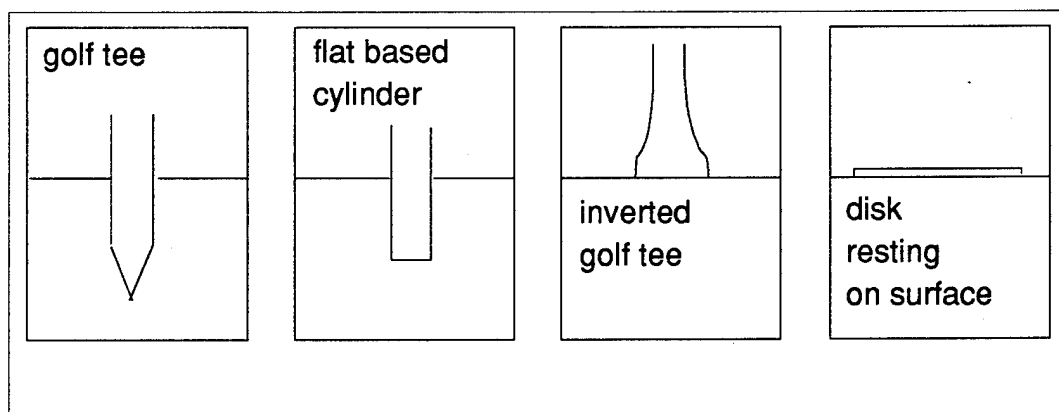


Figure (1.4) Receiver ground coupling methods

The golf tee allowed for the greatest sensitivity however the received amplitude varied by greater than five percent. The inverted golf tee resting on the surface with approximately 20 grams of mass loading on a ring element reduced variations to within five percent. This coupled with signal averaging discussed later gave marginally repeatable results. However, the results were not considered satisfactory. Further tests were done using a commercial single axis geophone made by Halliburton Geophysical Services, model number S4408A. Though these geophones were not as sensitive as the various piezo-electric sensors, they were found to be more reliable in producing repeatable data.

#### **E. SUPPORTING EQUIPMENT**

The layout of the test tank and supporting equipment is shown in Figure (1.5). The setup consisted of five elements:

1. The redwood tank filled with sand.
2. Support equipment above the tank.
3. Lab instruments including:
  - a. An HP 3314A Function Generator which was used as a source function generator for attenuation measurements and to characterize cylindrical spreading. It was also used to provide a reference signal when designing the array function generator visual instrument (vi) created in LabVIEW.
  - b. An COS 6100A Oscilloscope to visually monitor analog

input and output signals.

c. An HP 3562A Dynamic Signal Analyzer was utilized to isolate optimal propagation frequencies for given conditions.

d. An Ithaco 1201 Low Noise Preamplifier was used to filter and amplify to the received signal.

e. A Techron 5507 Power Supply amplified the source signal.

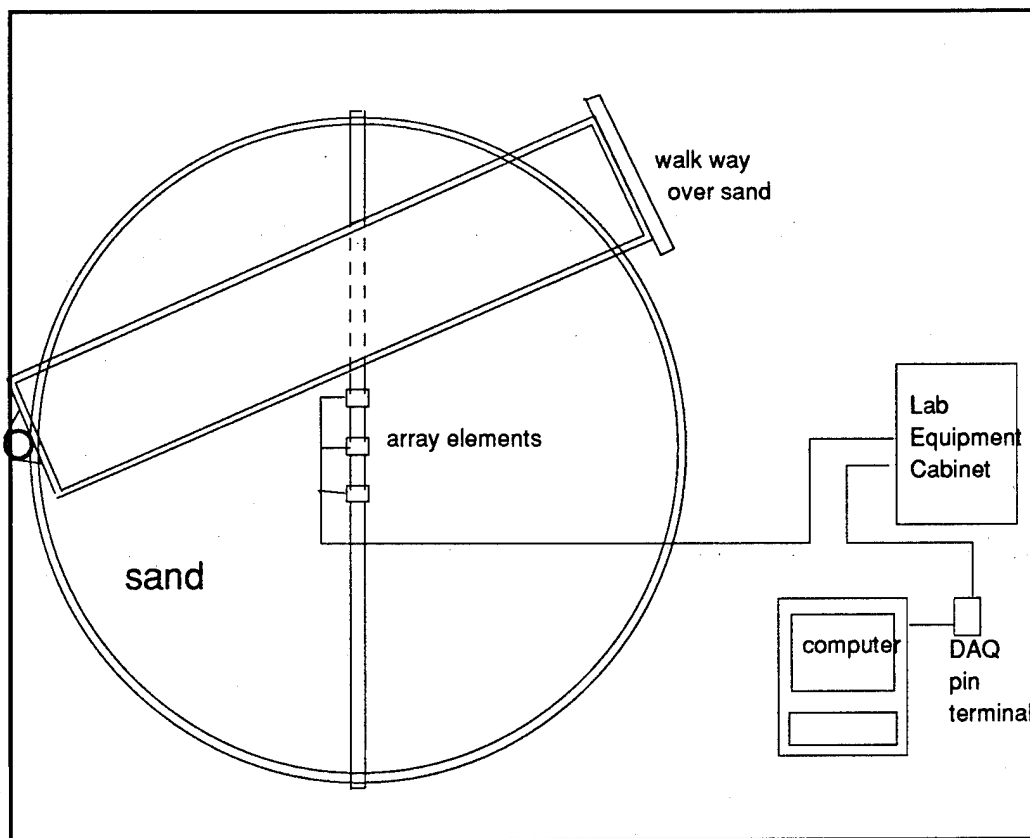


Figure (1.5) Lab set-up.

4. A Macintosh IICI computer with a LabVIEW interface board provided data acquisition.
5. Sources and receivers

## **F. DATA AQUISITION SYSTEM**

It was decided to perform data acquisition functions with LabVIEW. The data acquisition functions are implemented through software visual instruments or vis. The various vis used in this research are explained later and in the appendixes. The vis allow pulse generation, signal averaging, filtering, A/D conversion, and a high data recording rate. In addition to the software, two plug-in board were needed, the NB-MIO-16XL Data Aquisition board and the NB-AO-6 Analog Output board.

### **III. CHARACTERISTICS OF A POINT SOURCE**

The first step toward building a phased array surface wave source is to have well characterized single sources. The purpose of this chapter is to discuss the characteristics of the waves generated by a single source. First, we examine the radial and azimuthal dependence of the wave for different frequencies. Next, results are presented of scattering measurements from a buried target. Finally, we discuss target localization using multiple receiver, bistatic scattering.

#### **A. RADIAL DEPENDENCE**

The purpose of measuring the radial dependence of the wave propagation is threefold: 1) to determine if the medium is isotropic, 2) to determine if the waves spread cylindrically, and 3) to determine the attenuation coefficient for later use in calculating beam patterns for the phased array.

##### **1. Procedure**

The point source was mounted on the beam in the middle of the tank after the sand had been wetted uniformly. Test points were laid out every 10 cm along two lines, oriented at right angles. The HP 3314A Function Generator was used to generate a single cycle pulse. This pulse was amplified with the Techron 5507 Power Supply and sent to the driver. The received signal was sent to the



the Ithaco 1201 Low Noise Preamplifier to be amplified and filtered. The signal was then recorded using the Intensity Field vi as

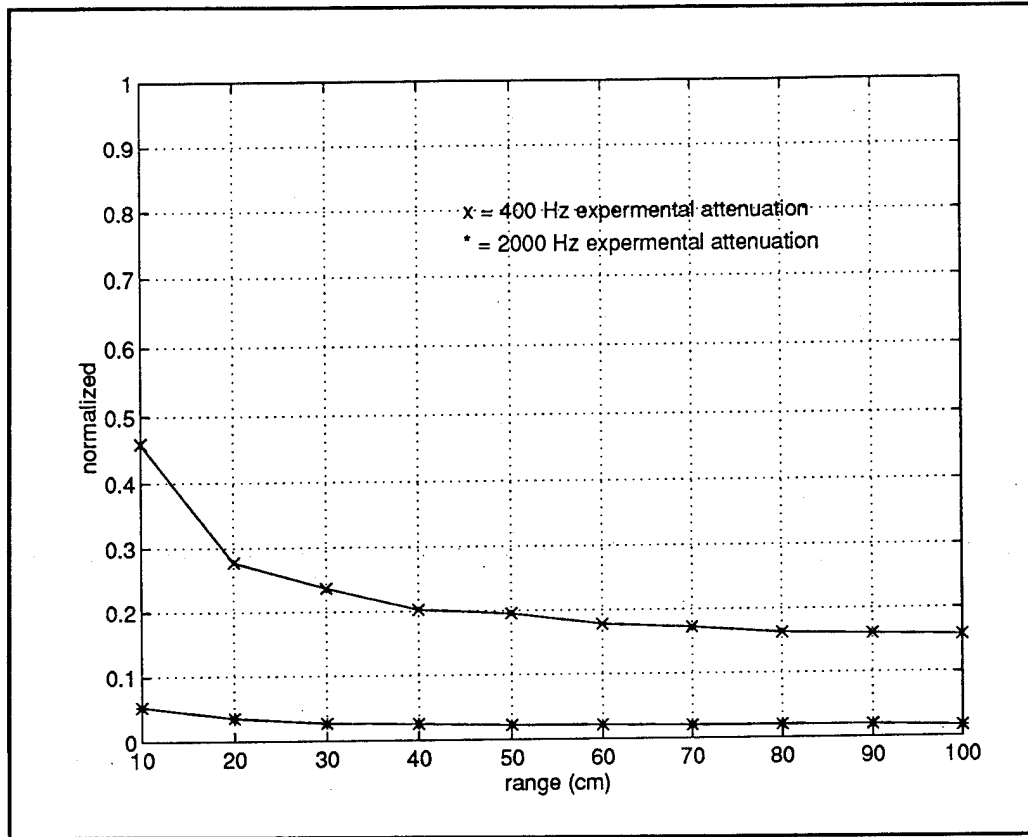


Figure (3.1) Attenuation in sand.

shown in Figure (3.3). Measurements were taken from the outer radial distance moving toward the source in order not to disturb the sand associated with successive measurements. As can be seen from the graph, Figure (3.1), the signal decreases monotonically with range. To determine whether the spreading is cylindrical and the value at the attenuation coefficient ( $\alpha$ ), the measured amplitude is compared to its assumed functional form [Ref 6]:

$$y = A / \sqrt{r} * e^{-\alpha r} \quad (1)$$

Dividing the amplitude at  $r$  by that at a range  $r_o$  gives:

$$y = y(r_o) * \sqrt{r_o / r} * e^{-\alpha(r-r_o)} \quad (2)$$

Rearranging and taking the natural logarithm results in

$$\ln(\sqrt{r / r_o} * y / y_o) = -\alpha(r - r_o) \quad (3)$$

The slope related to the value of the attenuation coefficient, has a value of 2.44 dB/m which compares with results for similar shear waves derived by N. P. Chotiros, [Ref 8], for sand, Figure (3.3). By

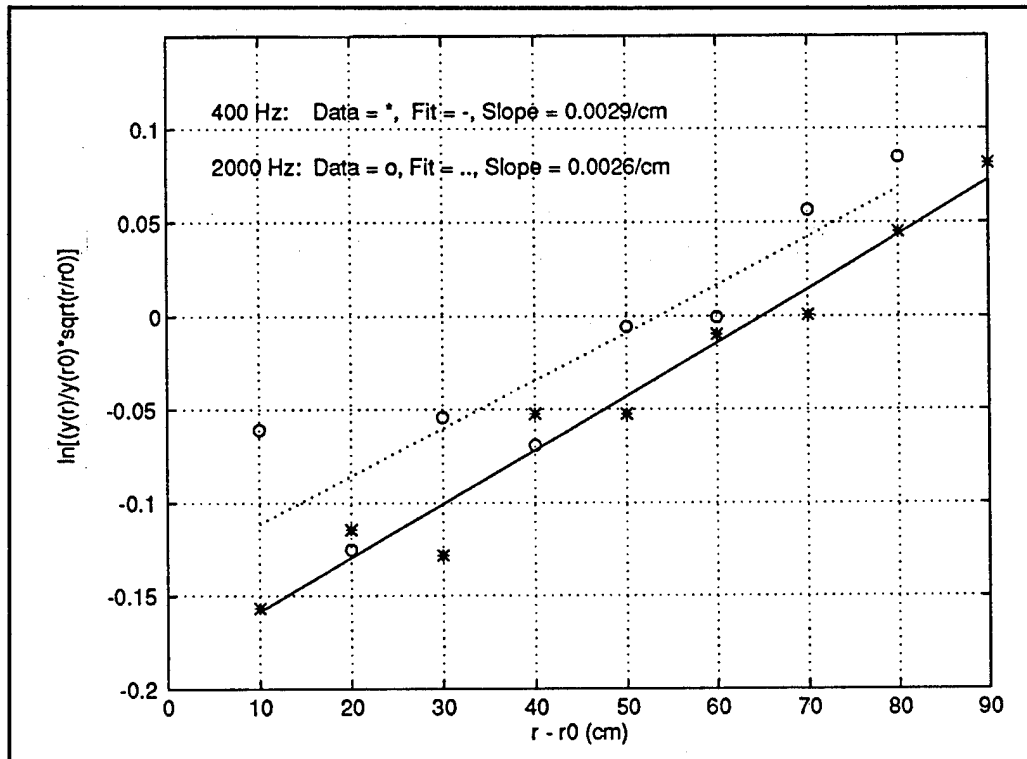


Figure (3.2) Value of attenuation coefficients.

plotting the data in this form, we can see that data should fall on a straight line with slope  $-\alpha$ . The results for two different frequencies are shown in Figure (3.2).

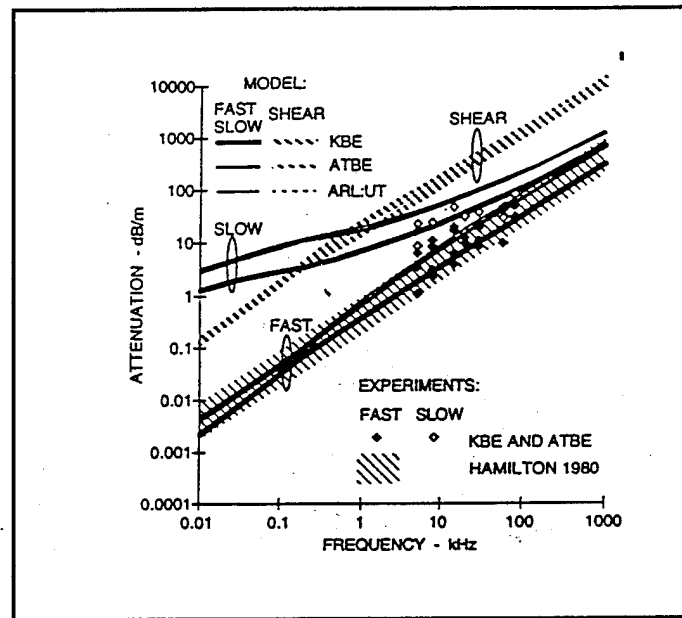


Figure (3.3) Attenuation measurements by Chotiros.

## B. AZIMUTHAL DEPENDENCE

Having investigated the radial dependence of the wave amplitude, the next step is to investigate the azimuthal dependence.

### 1. Procedure

To insure relatively consistent conditions, the tank was watered and allowed to settle for 30 minutes to improve moisture uniformity. The source was put in place, and measurements were taken as rapidly as possible. Measurements were taken at one meter range with thirty degree separation between locations. Data was

acquired using the vi illustrated in Figure (3.4), and a programming diagram in Appendix (B). This vi was designed to receive voltage amplitude triggered on the outgoing pulse of the HP3314A function generator and average a specified number of pulses to improve consistency in measurements. The results, for 400 Hz and 2000 Hz, shown in Figure (3.5), show that the spreading, was roughly uniform in all directions. It is interesting to note that these measurements were taken utilizing a one cycle pulse. Increasing the pulse length showed greater consistency in the received signal amplitude but created a larger problem with reflection off the walls of the tank. The results of the measurements, though not ideal, were considered adequate to attempt beamforming utilizing an array.

### **C. SCATTERING FROM A BURIED OBJECT**

An evaluation of scattering from a buried object was conducted using a single source and multiple receiver set-up to evaluate the feasibility of using an array. This was accomplished by placing the source at the center of the tank and three receivers at approximately one meter ranges at various bearings out from the source. A vi, Figure (3.6), with a diagram and explanation in Appendix (C), was designed to acquire the received signal triggered on the source pulse and average it over a specified number of pulses. The averaged received signal was then saved, on a ten centimeter diameter, three centimeters thick, copper cylinder object placed in the tank covered by two centimeters of sand. The procedure was

repeated and the second averaged signal was subtracted from the first using the  $v_i$  in Figure (3.7), with a diagram and explanation included as Appendix (C). As can be seen in Figure(3.6), the arrival of the direct path and the reflected path are revealed in the time domain plot. By knowing the location of the source and the receiver, the speed of the Rayleigh wave can be determined from the direct path. The length of the reflected path can then be determined. This length specifies an ellipse, corresponding to possible locations of the object, Figure (3.8). By utilizing multiple receivers, an object can be located by finding the intersection of multiple ellipses. This was accomplished with the data shown in Figures (3.9, 3.10, 3.11) and plotted in Figure (3.12). The location of the source and three receivers are indicated by the open circles. The location of the buried object is indicated by the x. It is seen that the x is near the intersections of the ellipses. This technique must be developed further but the results are encouraging.

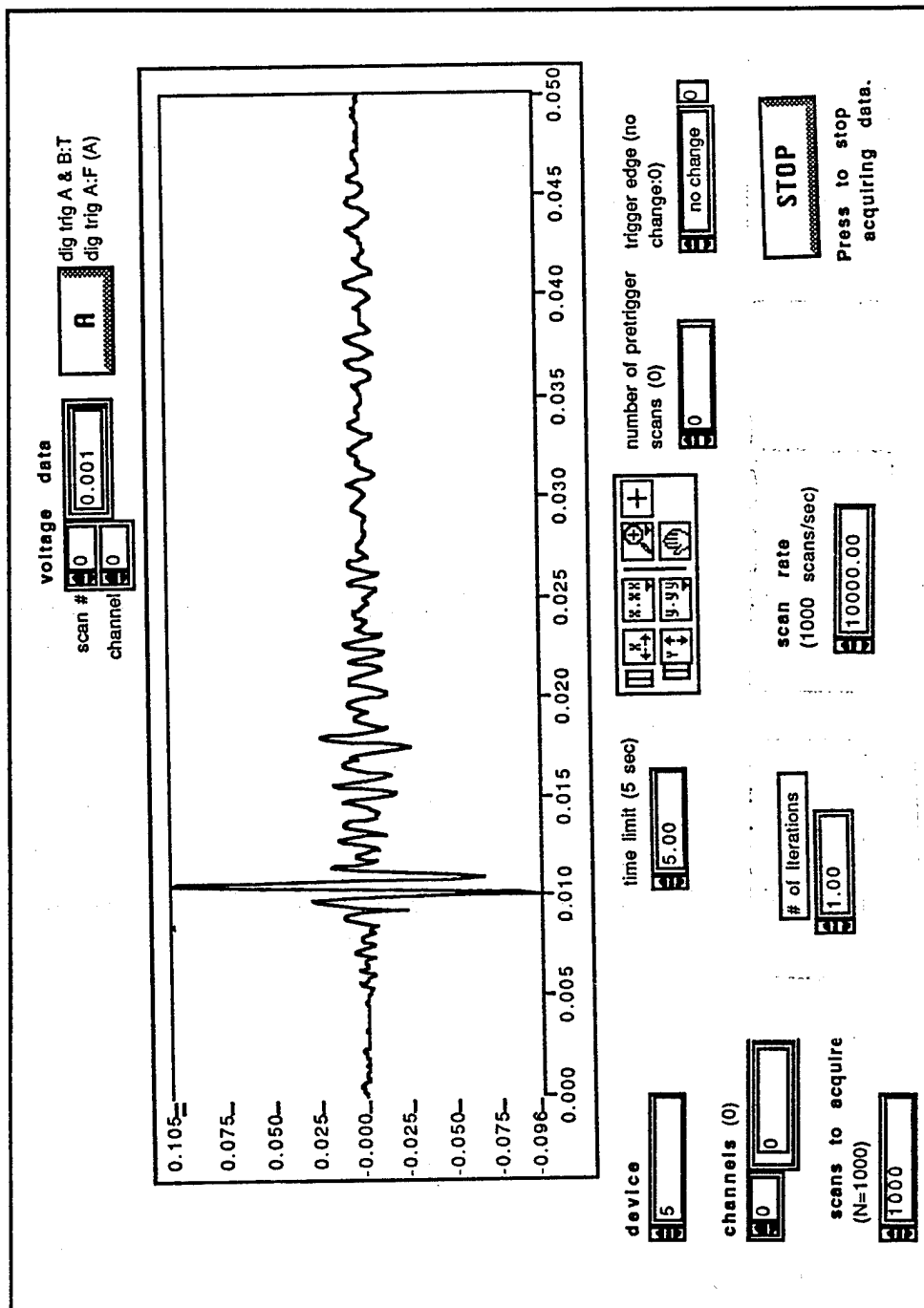


Figure (3.4) Front panel Intensity Field vi.

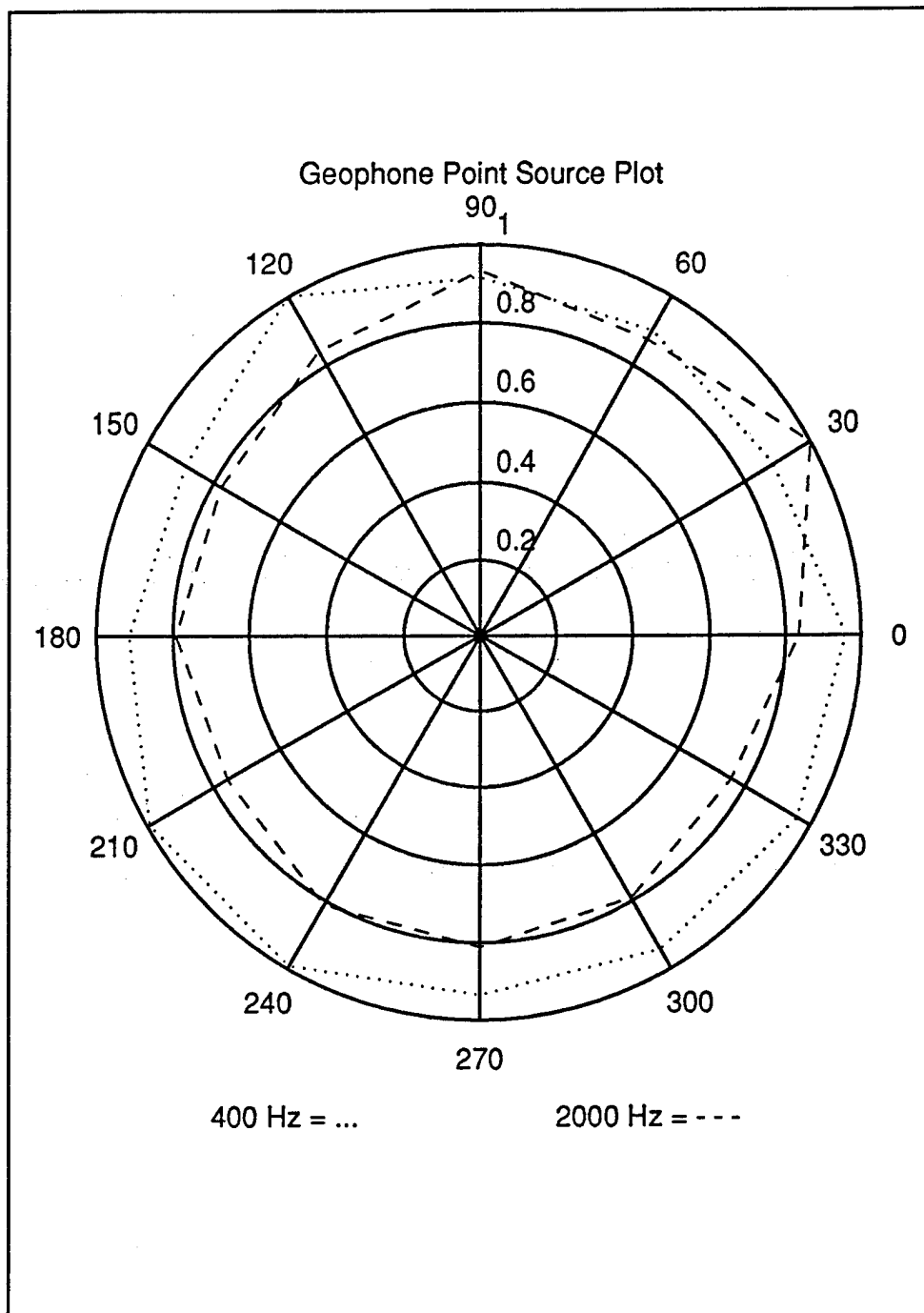


Figure (3.5) Azimuthal dependence of waveform

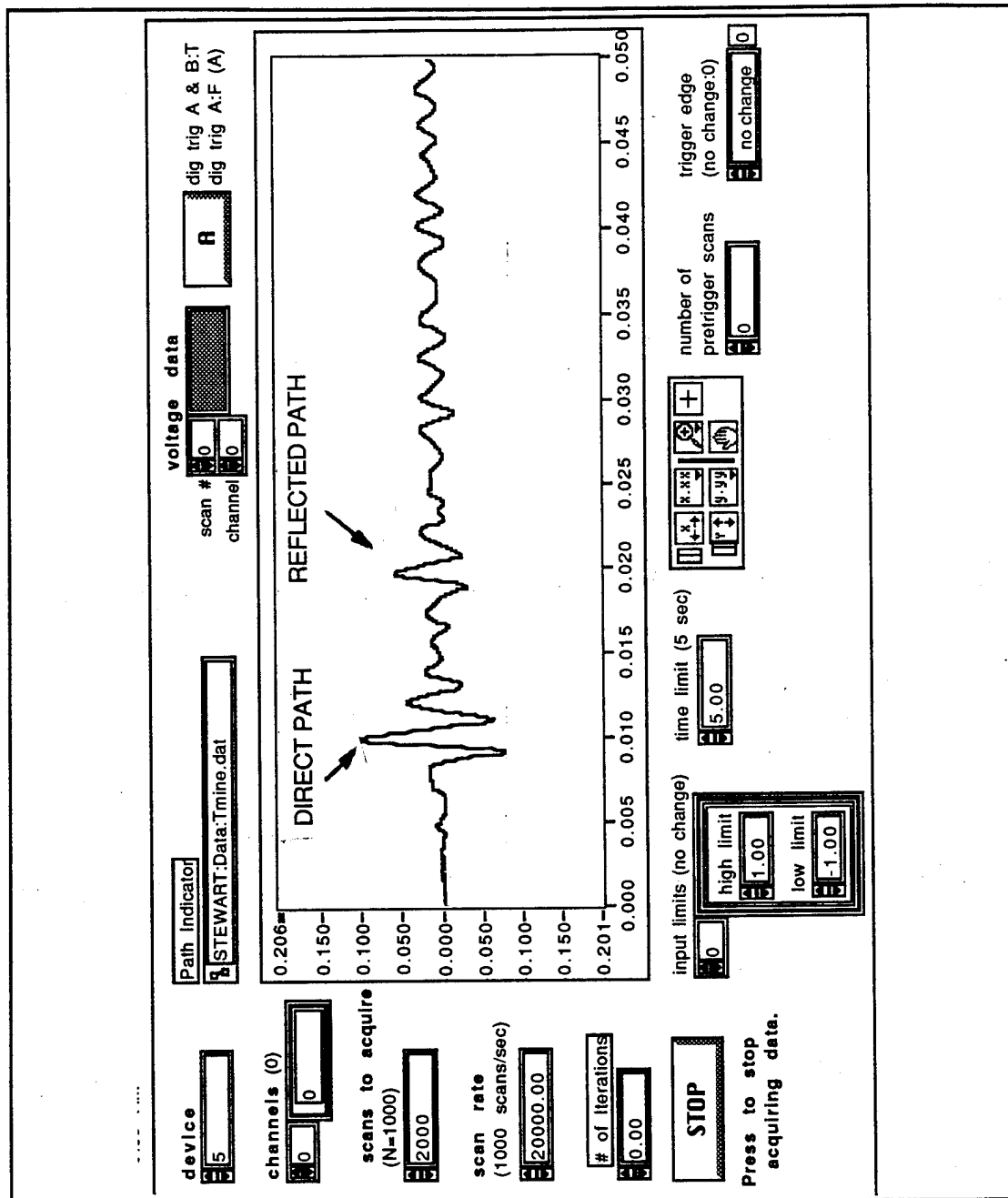


Figure (3.6) Signal Averaging vi.



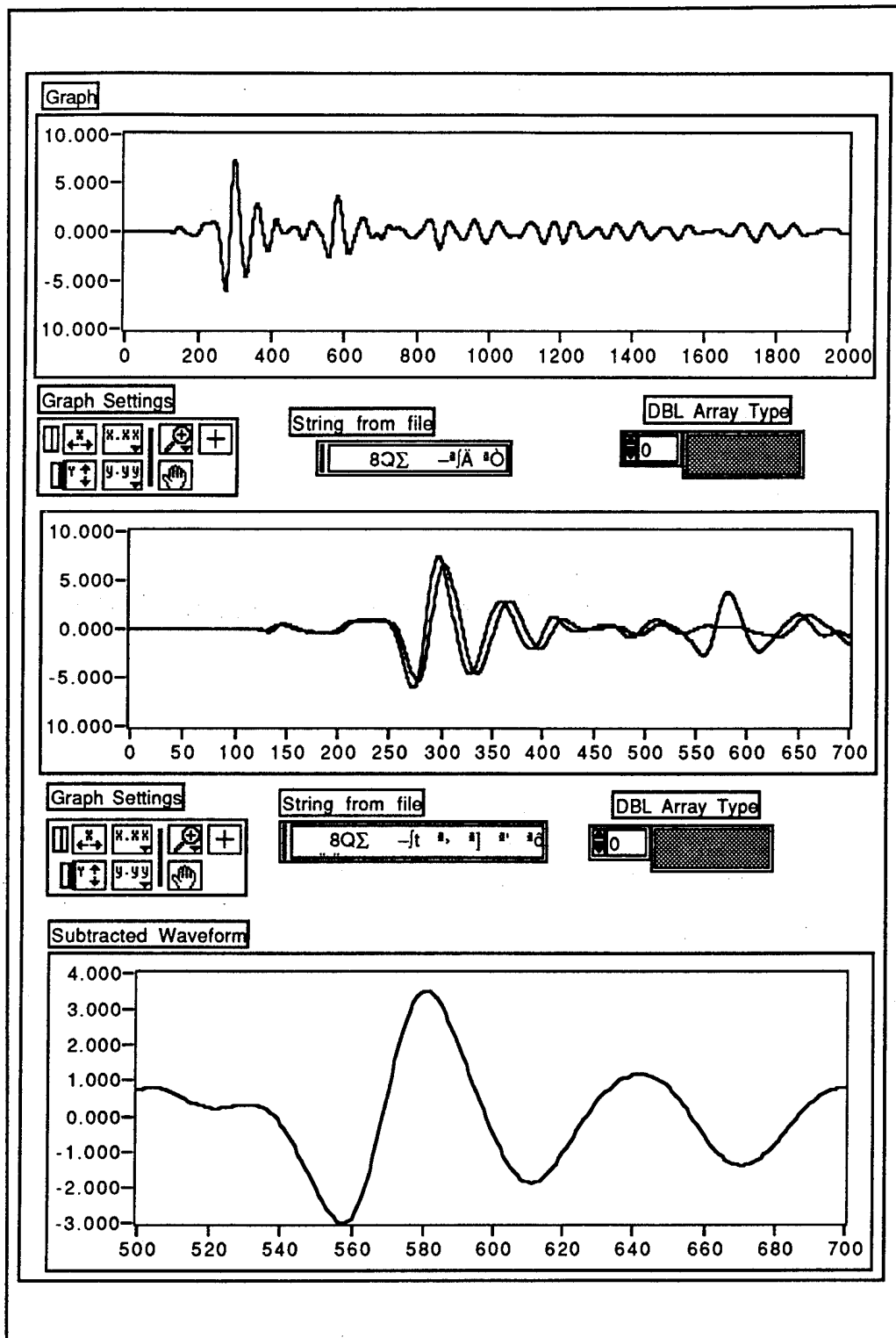


Figure (3.7) Front panel Comparison vi.

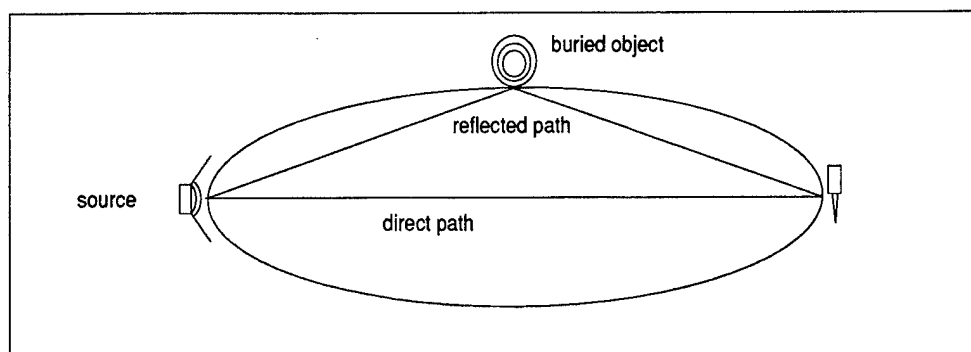


Figure (3.8). Ellipse determined by reflected path.

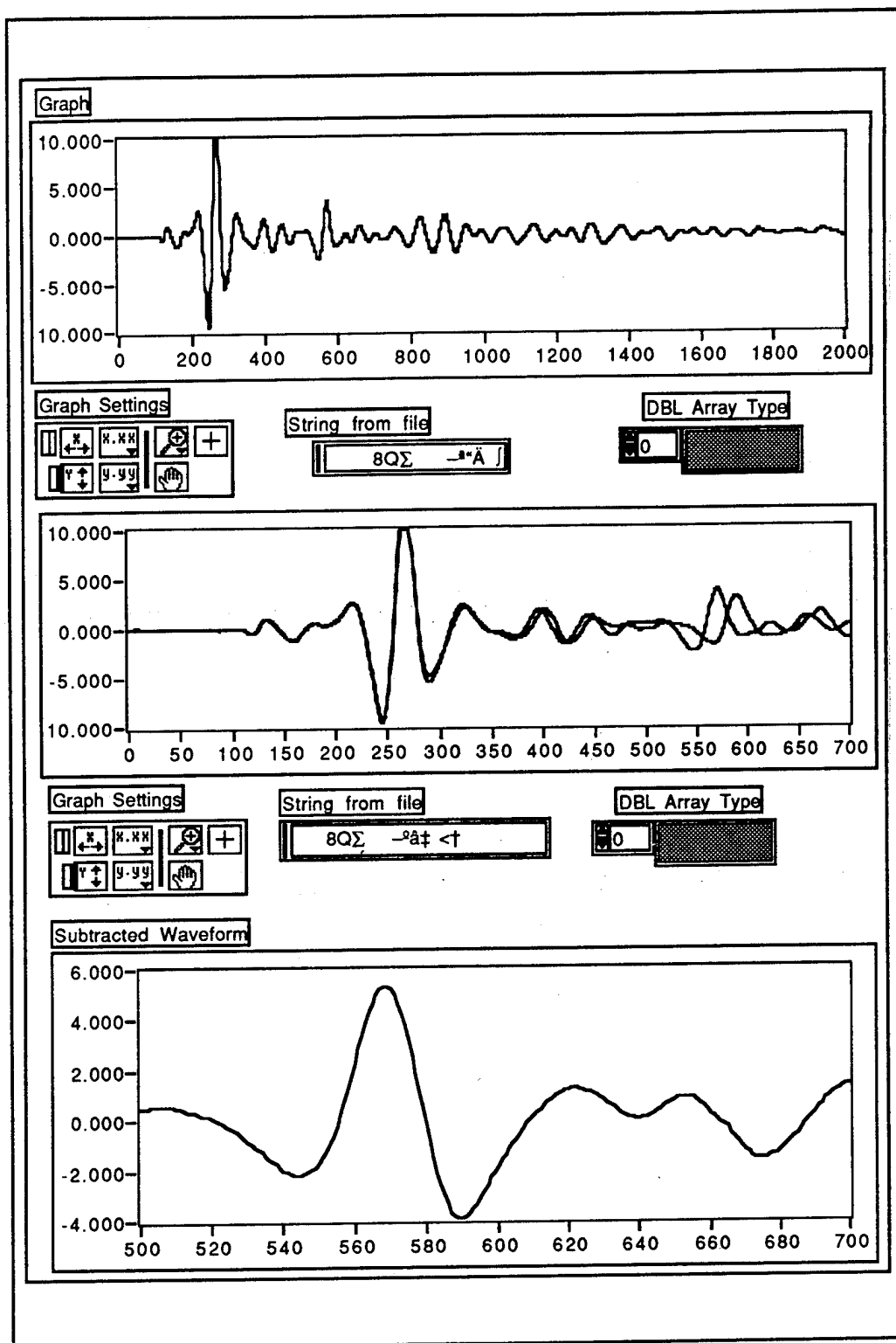


Figure (3.9) Comparison of 004 degree path.

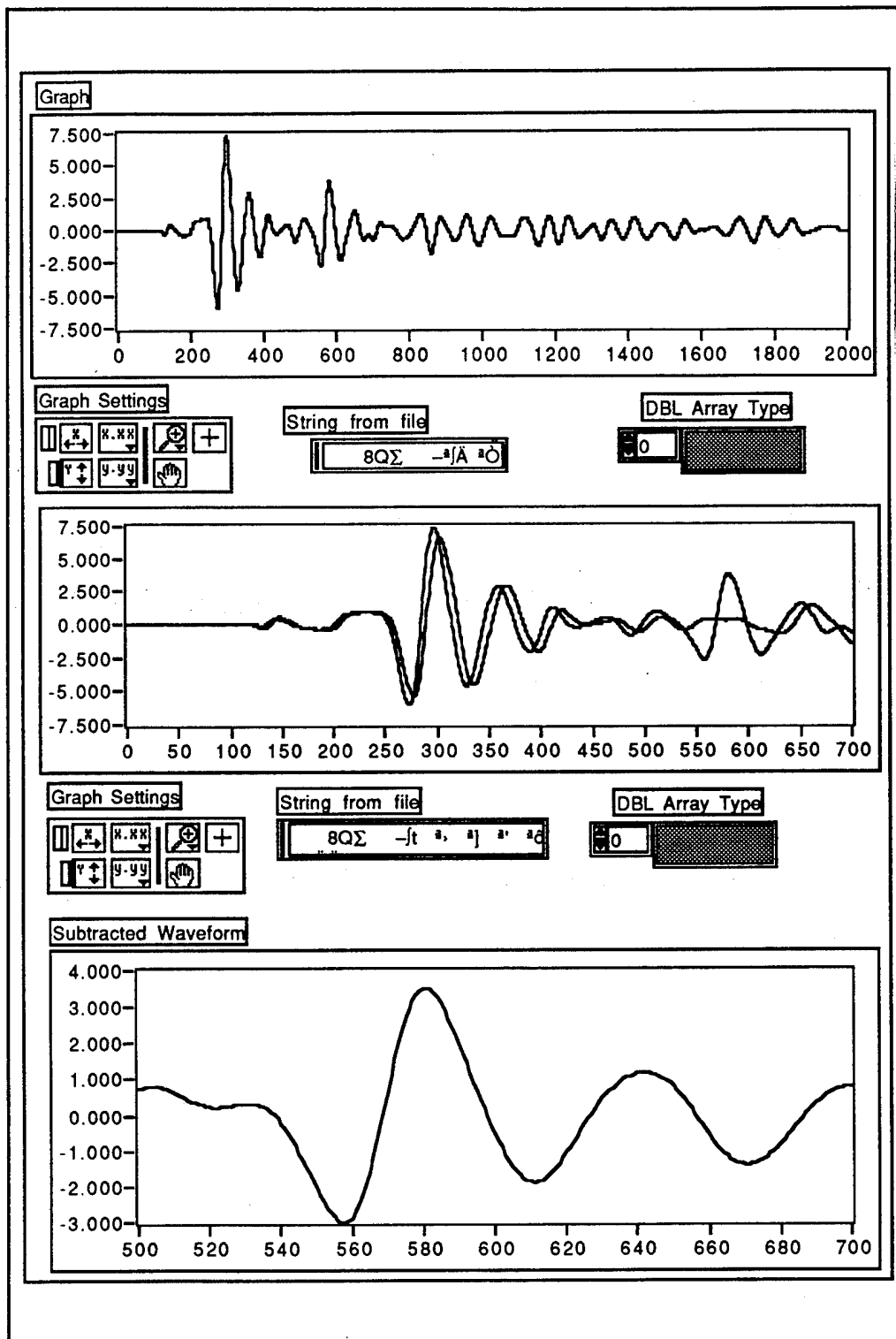


Figure (3.10) Comparison of 036.2 degree path.

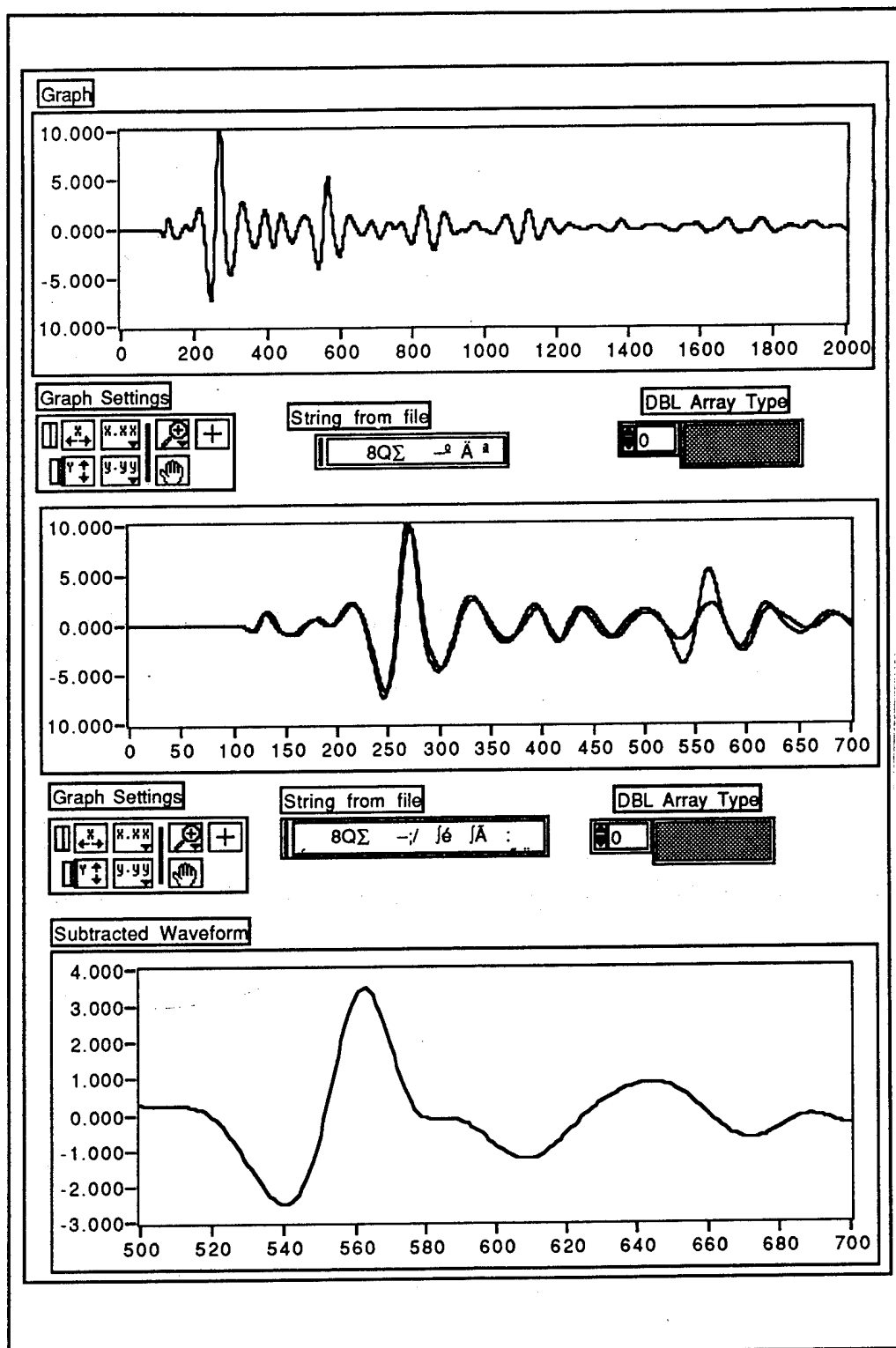


Figure (3.11) Comparison of 079 degree path.

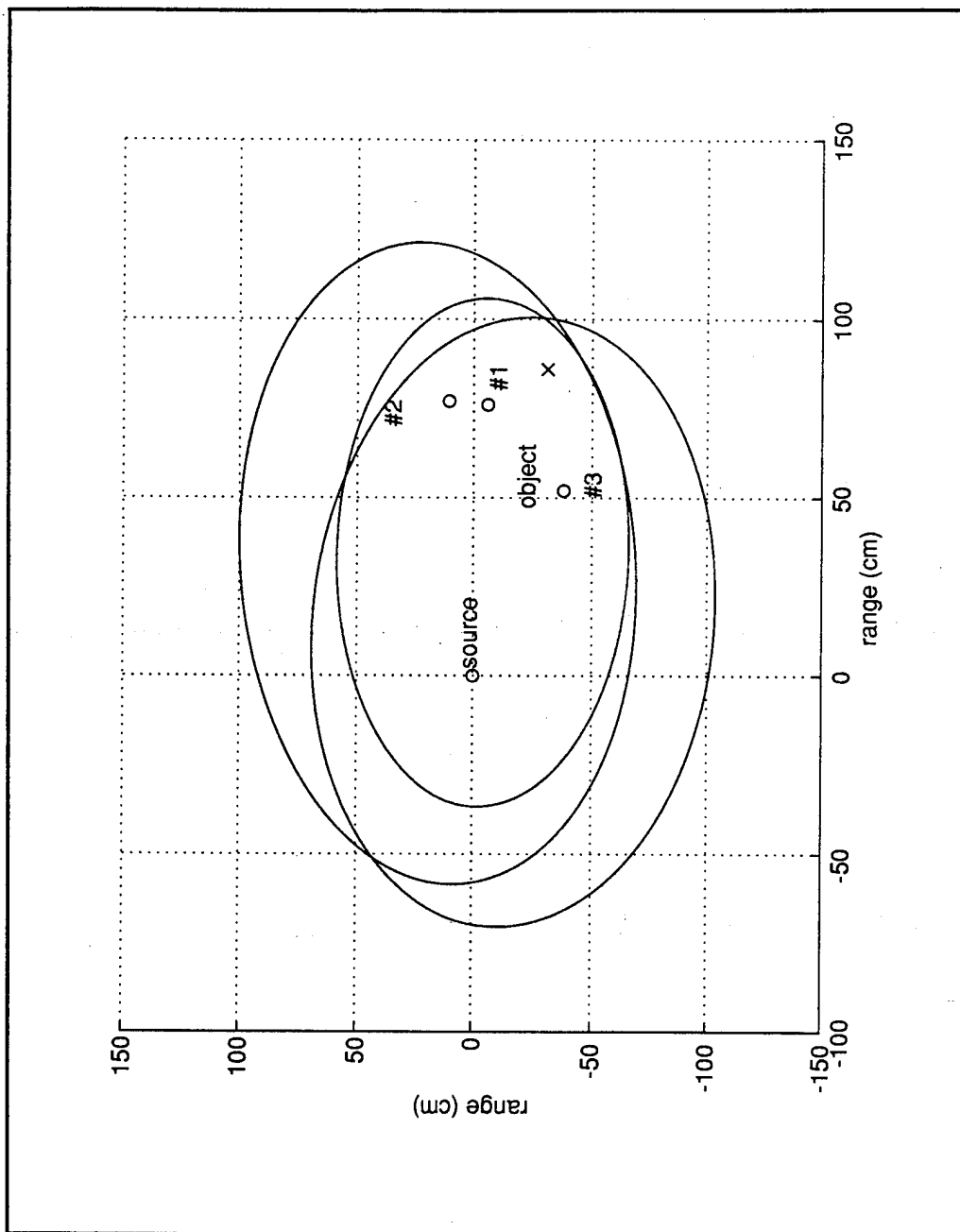


Figure (3.12) Plot of elliptical paths.



## IV. PHASED ARRAY BEAMFORMING

Having investigated the single point surface wave source, attention is now turned to an array of sources.

### A. BEAMFORMING

To investigate the feasibility of beamforming required some changes to the lab set-up. A three-element array configuration was selected, which required two additional sources to be built. Because the NB-MIO-16XL DAQ card can only support two analog output channels, a NB-AO-6 analog output card was acquired providing additional analog output channels. This addition enabled the use of a multichannel analog output control vi for the array.

### B. BEAMFORMING MODEL

To predict the beam pattern, a model was derived based on the simple line array [Ref 5]. A line array of  $N$  simple sources spaced by a distance  $d$ , having the same amplitude and phase will generate a velocity of the form

$$v(r, \theta, t) = \sum_{i=1}^N \frac{A}{\sqrt{r_i}} e^{j(\omega t - k r_i)} \quad (4)$$

where  $r_i$  is the distance from the  $i^{th}$  source to the receiver at  $(r, \theta)$ . A program written in MATLAB, Appendix (D), produced a plot of the beam pattern based on the number of elements, their spacing,



amplitude weighting and phase. The results of this program are compared with the results acquired in the sand tank.

### C. EXPERIMENT

The experiments were designed so as to allow comparison with the beamforming model. Phasing and weighting for each element were identical in the initial experiment. To evaluate the ability to beamform, the three elements of the array were fixed on the cross beam while the receiver was free to move azimuthal at fixed range from the center element. The Beamforming vi utilized, Figure (4.1), diagram Appendix (E), allowed for independent control of each element in frequency, phase, amplitude and pulse width to a high degree of accuracy. Though not utilized to its full capacity during these initial experiments, it is able to support more complex array analysis.

In the first experiment, the spacing was set to one wavelength ( $\lambda = .18$  meter) having measured a corresponding surface wave speed ( $c = 61.2$  m/s) at a frequency of 340 Hz. The drive voltage and phase were equal for all elements. The pulse length was adjusted to fifteen cycles to allow for sufficient overlap of the signals from the three sources to produce interference. Figure (4.2) shows the received waveforms at eight selected bearings, arranged in approximately the correct orientation. The center plot represents a typical waveform received at bearings

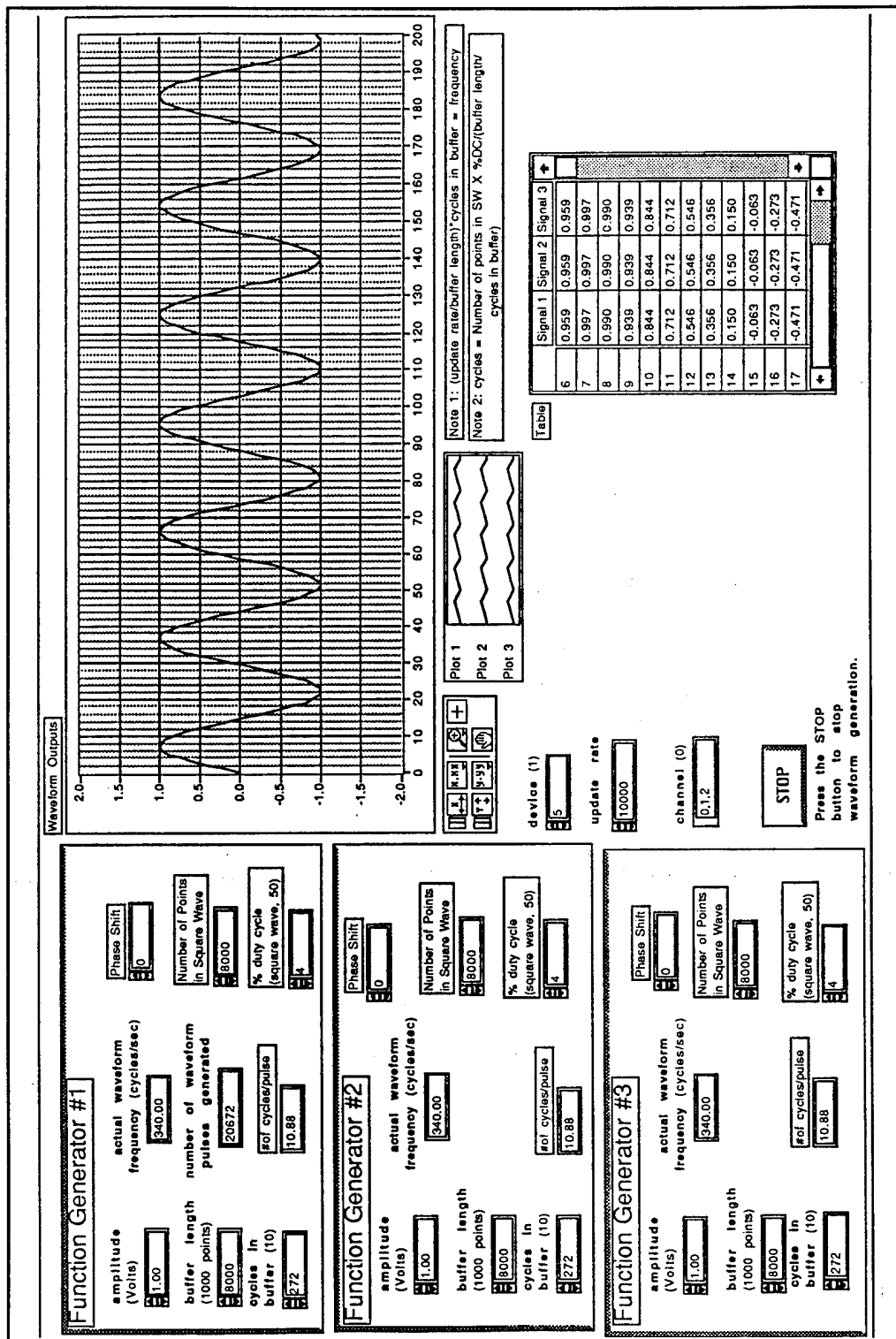


Figure (4.1) Beamforming vi Front Panel.

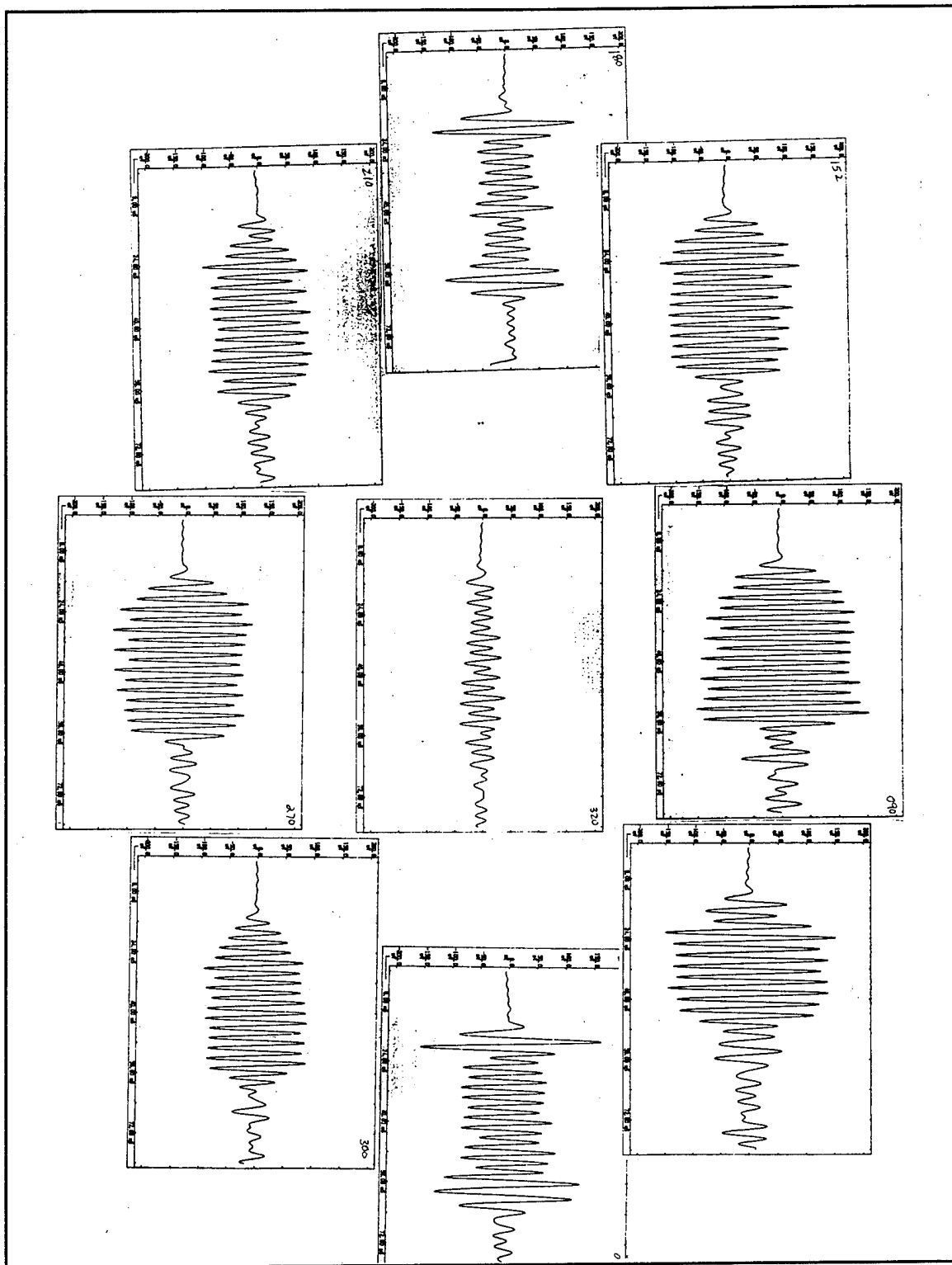


Figure (4.2) Received pulses at indicated bearings.

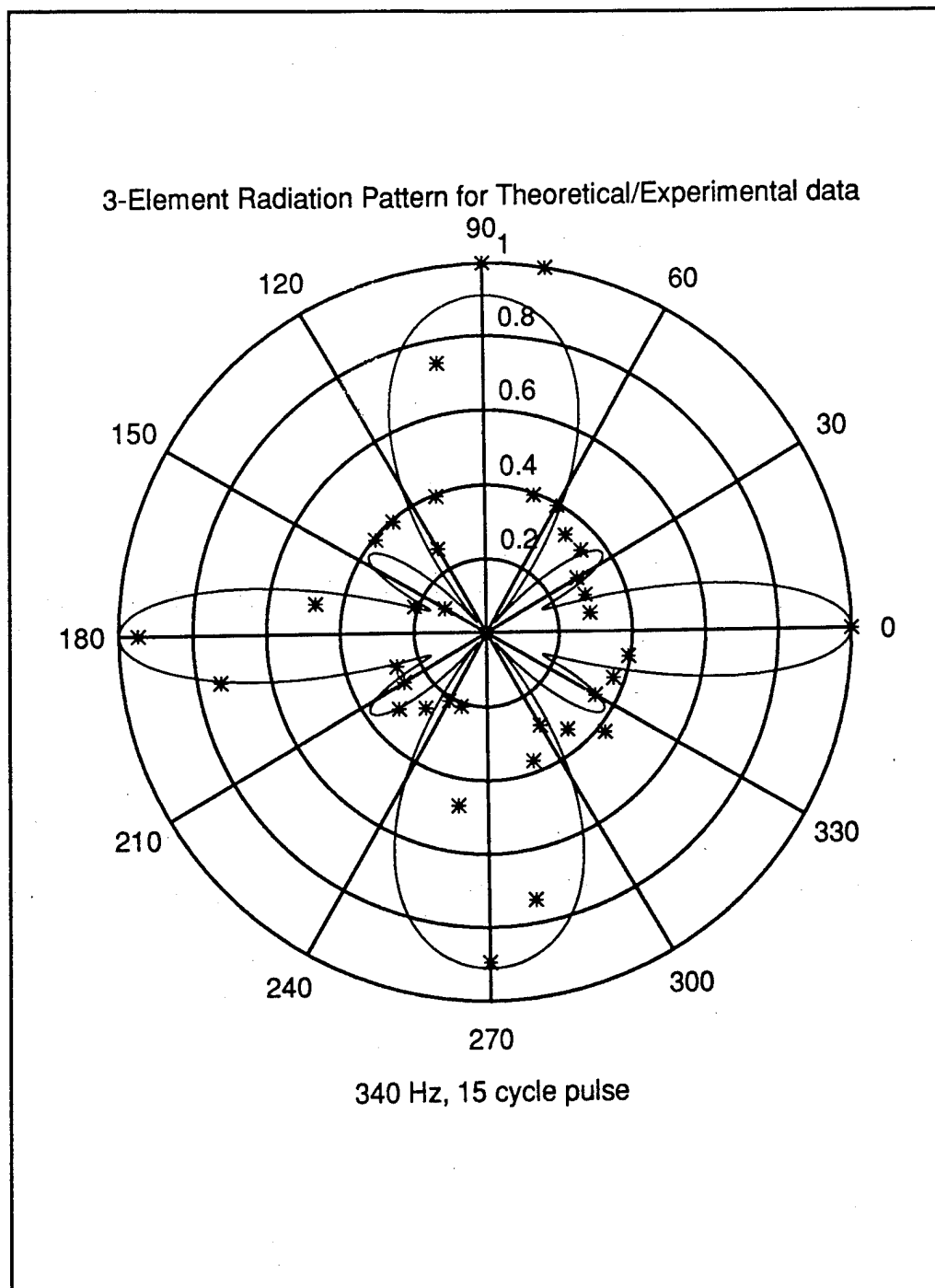


Figure (4.3) Calculated beam pattern for three element array overlayed by experimental data.

centered between the other locations. The variation in amplitude from bearing to bearing, and the symmetry about the axis demonstrates the beamforming. When compared to the theoretical beam pattern, Figure (4.3) it is seen that the array is producing the correct radiation pattern. Figure (4.4) shows the effect of beamforming at a specific bearing. The upper figure is the signal from a single source, the lower is the signal with all three sources driven. Clearly beamforming works.

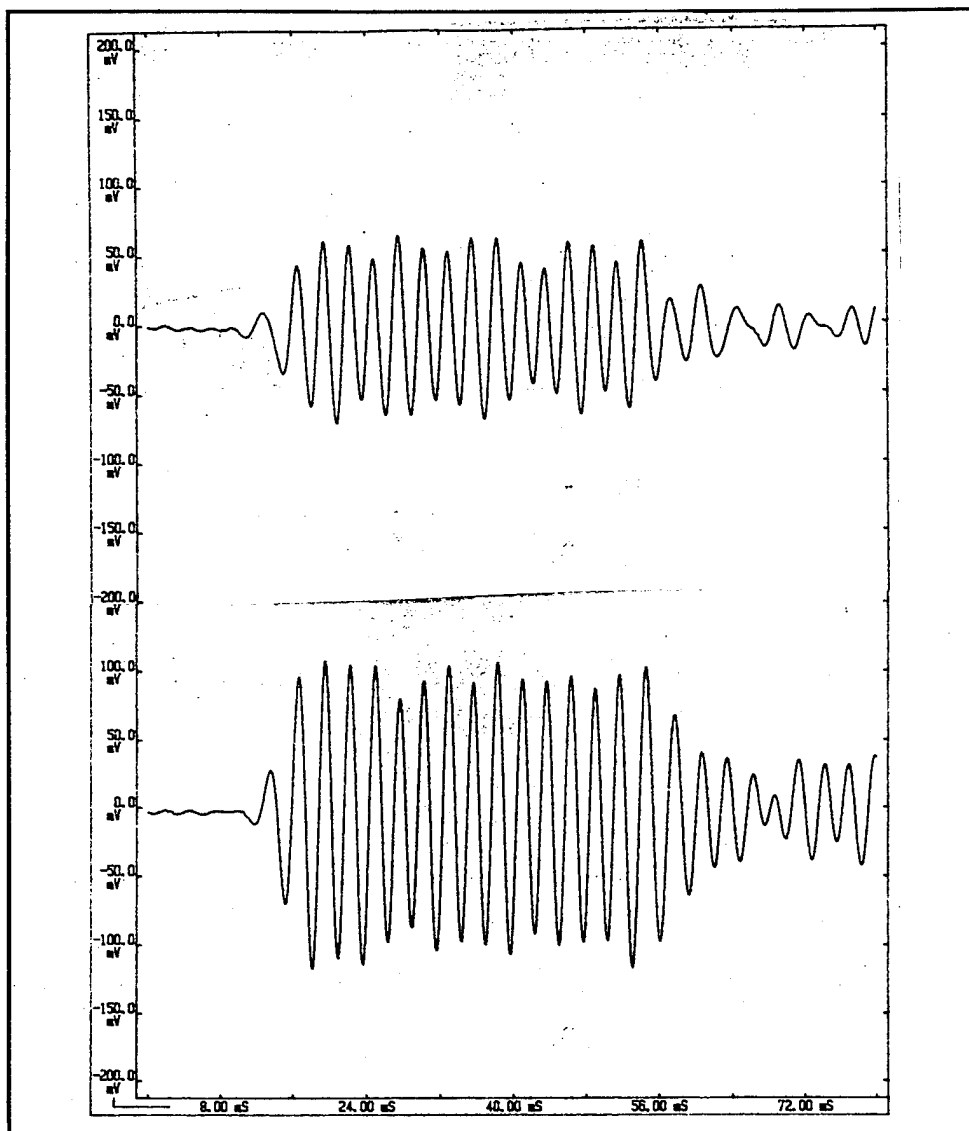


Figure (4.4) Signal with and without beamforming.



## **V. CONCLUSION**

### **A. RESULTS**

The results of this research are encouraging. We successfully demonstrated target localization using surface wave scattering and beamforming with phased array technology. Further development of the system is recommended.

The size of the test tank proved to be a significant limitation. A next step would be to build a portable system that could be taken to the beach. Performing measurements at the beach will allow the use of longer ranges and lower frequencies. It will also provide realistic background noise.

Other recommendations are to investigate pulse shaping and more advanced signal processing techniques to address the issue of probability of detection, etc. This project is an ideal area to apply recent advances involving time reversal signal processing, [Ref 6].





## APPENDIX A. FACTSHEET ON SOURCE ELEMENT

A four inch woofer speaker manufactured by Radio Shack was selected as a source element. Keeping cost considerations in mind, it had excellent source element characteristics. The long cone excursion of flexible rubber provided the necessary pressure to maintain coupling with the ground. The dust cap was sturdy enough to support various attachments affixed without deforming. The backplate was a large flat area to allow for attachment of a mounting post, Figure (A.1).

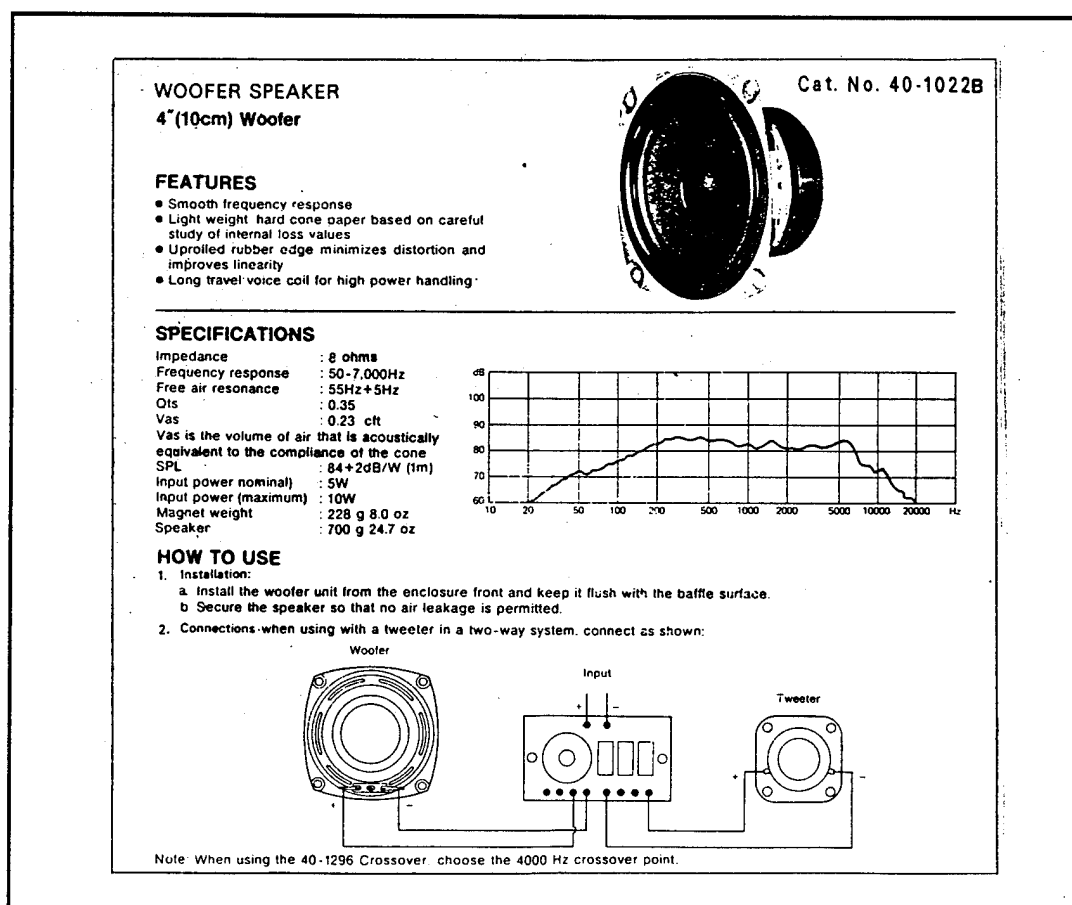


Figure (A.1) Factsheet on source element



## APPENDIX B. LABVIEW VI FOR INTENSITY FIELD STUDY

The purpose of this vi is to take field intensity measurements to determine attenuation and to measure spreading. The vi is designed to be triggered by the HP 3314A Function Generator, acquire a specific number of received wave forms and average them. The three programming elements necessary were a "for loop," shift registers and an intermediate vi call AI wave. The three

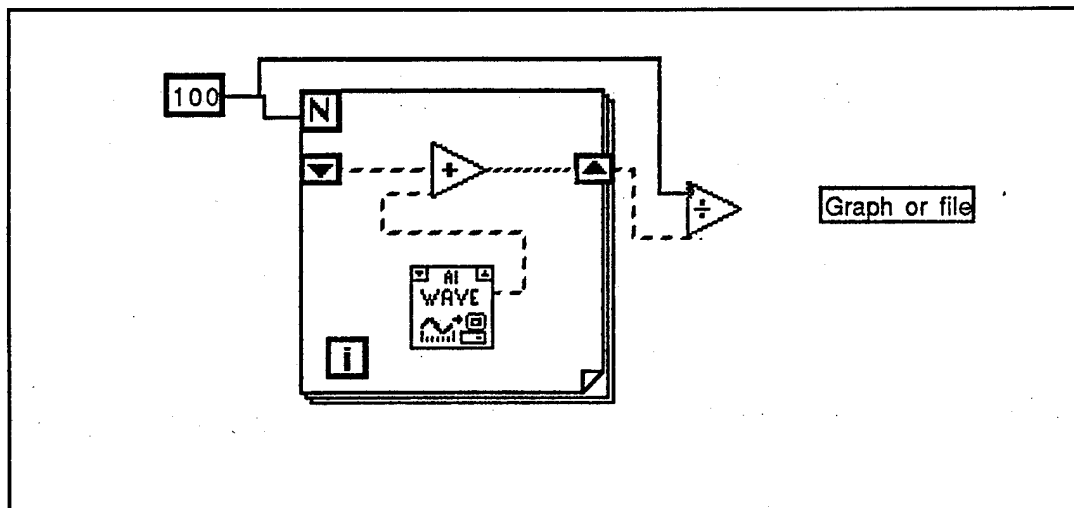


Figure (B.1). Elements of Intensity Field vi.

elements can be seen in the simplified version above, Figure (B.1) and as elements of the actual program in Figure (B.2). The block is a "for loop." The arrows on each side are the shift registers. The AI WAVE vi which acquires the signal is also shown. In this case the "for loop" value is 100. Therefore, 100 acquisitions are made, summed and then divided by the "for loop" value to get an average of the

signal. The shift registers are used to carry the summed value to the beginning of the loop until the "for loop" value is reached. This is a timed acquisition, meaning that a hardware clock is used to control the acquisition rate. It is also a buffered acquisition, meaning that the data is stored in an intermediate memory buffer after it is acquired from the analog input channel. On the left side of the vi, in the lettered boxes, Figure (B.2), are the front panel inputs controlling the number of iterations, device, channel input, trigger type, and scan information.

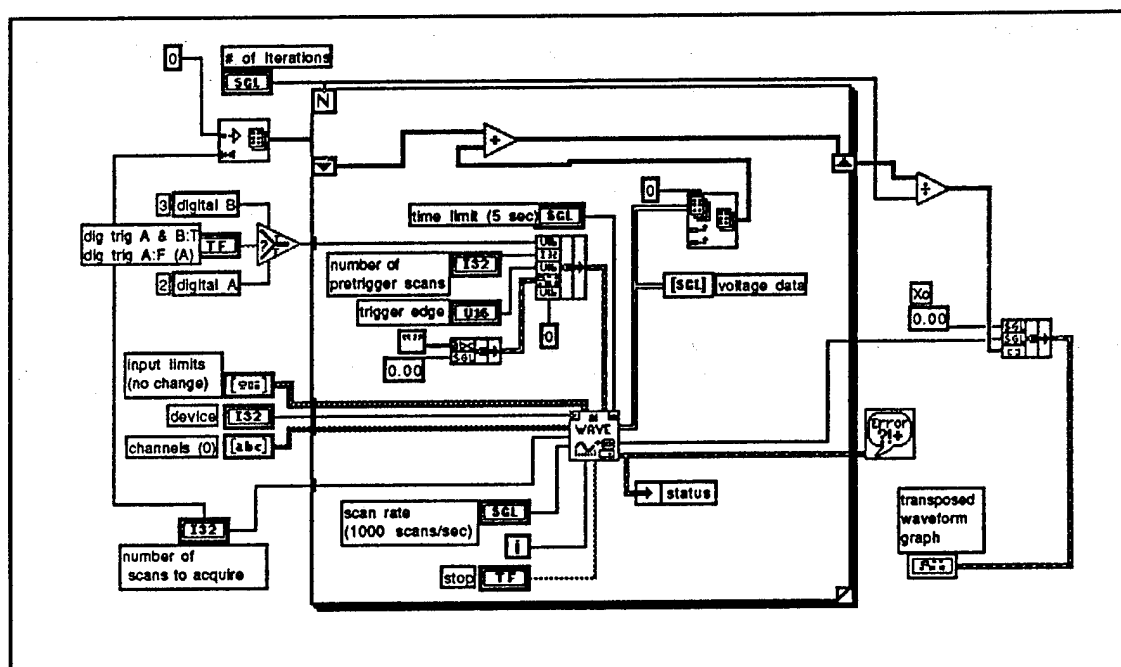


Figure (B.2) Field intensity vi.

## **APPENDIX C. LABVIEW VI'S FOR DATA ACQUISITION**

Two vis were used to acquire and analyze data to determine object location in the sand by surface wave sattering. The initial aquisition vi was similar to the vi used to take field intensity measurements except it created a binary file that could be used by a comparison vi. To create this file an addition was made to the field intensity measurements vi as shown below, Figure (C.1). This can be seen in the vi on the far right of Figure (C.2).

The comparison vi was written to read two binary files, displaying the first in the upper graph, both sets of points in the second graph, and the difference of the two in the third graph. In this way the additional disturbance in the field could easily be located in the time domain as shown in earlier Figures (3.9,3.10,3.11).

Once the arrival times for the direct and relected paths had been determined, a plotting program written in MATLAB was created to plot the ellipses with a known distribution. This allowed for generating points having the highest probability for object detection.



## APPENDIX D. MATLAB PROGRAM FOR ELLIPSE PLOTTING

As shown in Figure (3.8), it is possible to create a set of points that represent all the possible location of the target given the arrival time of the reflected and directed path. Using MATLAB, a program was developed to generate a set of ellipses representing multiple receivers. The program relies on the inputs provided by the user shown seen in the first few lines below:

```
%Ellipse Plotting of Scattering
%Create it so the input radial angle is the axis for the ellipse
%Angle can be input converted to x, y coordinates
home
clear
clg

%Receivers
for R=1:3;    %total number of receivers
    bearing = input('Enter the bearing to the Receiver ');
    range = input('Enter the range to the Receiver ');
    TT = input('Enter Travel Time of Reflected Path ');
    T = input('Enter Travel Time of Direct Path ');
    A = range*sin((pi/180)*bearing);
    B = range*cos((pi/180)*bearing);
    xo = A/2;    %center of ellipse
    yo = B/2;    %center of ellipse
    delT = TT-T;    %difference in travel times
    foc = range/2;    %center to foci distance
    C = range/T;    %wave speed based on direct path
    D = C*TT;    %distance traveled by reflected path
    by = sqrt((D/2)^2 - foc^2);    %minor axis
    ax = D/2;    %major axis
    t=0:.01:2*pi;
```



```

a=ax*cos(t);    %ax is 1/2 length of ellipse
b=by*sin(t);    %by is 1/2width of ellipse
X=(a)+xo;        %xo is center in x dir
Y=b;            %yo is center in y dir
Z = X+Y*i;    %z=X+Y*i
Zp(R,:)= Z * exp(i*(pi*(0.5-(bearing/180))));

end
clc
disp('Pick Mine Coordinates off the graph!')
pause(5)
figure(1)
hold on
    for R = 1:3;        %Change for the # of receivers
        plot(Zp(R,:))
    end
plot(0,0,'o')
plot(76,-6,'o')
plot(77,10.3,'o')
plot(52,-38,'o')
plot(86,-31,'x')
hold off
text(2,2,'source')
text(80,-10, '#1')
text(70,35, '#2')
text(50,-50, '#3')
text(47,-22,'object')
xlabel('range (cm)')
ylabel('range (cm)')
grid
[K,L] = ginput(1)
clc
disp(['Mine is located at X = ',num2str(K),' and Y = ',num2str(L)])

```

## APPENDIX E. MATLAB PROGRAM FOR BEAM FORMING ARRAY

To accurately evaluate the three element array in it's ability to successfully beamform, a MATLAB program was written, with the help of Professor A. Atchley, Naval Postgraduate School. Given inputs of the distance to the receiver, spacing between elements, wavelength, and phase and amplitude for each element it accurately predicts the radiation pattern of the array in the XY plane. The following is the actual program listing:

```
% Plot program for 3 element beam forming in the far field

theta = (-pi:.01:pi);      %angles
r = 1;                     %Distance to receiver from center
d = .18;                   %Spacing between elements
kd = 0.9.*2*pi;            %wave number * d
k = kd/d;                  %wave number

% Source 1 is at the top, 3 is at the bottom.

f1 = 0*pi/3;               %phase control of element 1
f2 = 0*pi/3;               %phase control of element 2
f3 = -0*pi/3;              %phase control of element 3

a1 = 1;                    %amplitude of element 1
a2 = 1;                    %amplitude of element 2
a3 = 1;                    %amplitude of element 3

% Range from element to receiver

r1 = sqrt(r*r*cos(theta).*cos(theta) + (r*sin(theta) -
      d).*(r*sin(theta) - d));
r2 = r;
```

```

r3 = sqrt(r*r*cos(theta).*cos(theta) + (r*sin(theta) +
      d).*(r*sin(theta) + d));

% Pressure created by each element

p1 = a1*exp(i*(-k*r1 + f1))./sqrt(r1);
p2 = a2*exp(i*(-k*r2 + f2))./sqrt(r2);
p3 = a3*exp(i*(-k*r3 + f3))./sqrt(r3);

pabs = abs(p1+p2+p3);

pnorm = pabs./max(pabs);

%Experimental Data
Rdata = [380, 110, 110, 110, 130, 130, 150, 150, 380, 380, 280,
150, 100,...
150, 150, 50, 80, 180, 360, 280, 100, 100, 120, 100, 80, 80,
80, 340,...
280, 140, 110, 130, 160, 130, 140, 150, 380];
ttheta=0:pi/18:2*pi;
data = Rdata/380;
polar(theta,pnorm);
hold on
xlabel('375 Hz, 15 cycle pulse')
title('3-Element Radiation Pattern for Theoretical/Experimental
data');
grid;
polar(ttheta,data)
hold off

```

## APPENDIX F. LABVIEW VI FOR BEAMFORMING ARRAY

A LABVIEW vi was written to control the three element array. The basic design involved creating a sine wave of one cycle with a specific amplitude and frequency inside a "for loop" which generated multiple cycles. This was then multiplied by a square wave that had been created in a similar fashion. The results is a pulsed sine wave. These elements can be seen in the simplified version, Figure (F.1).

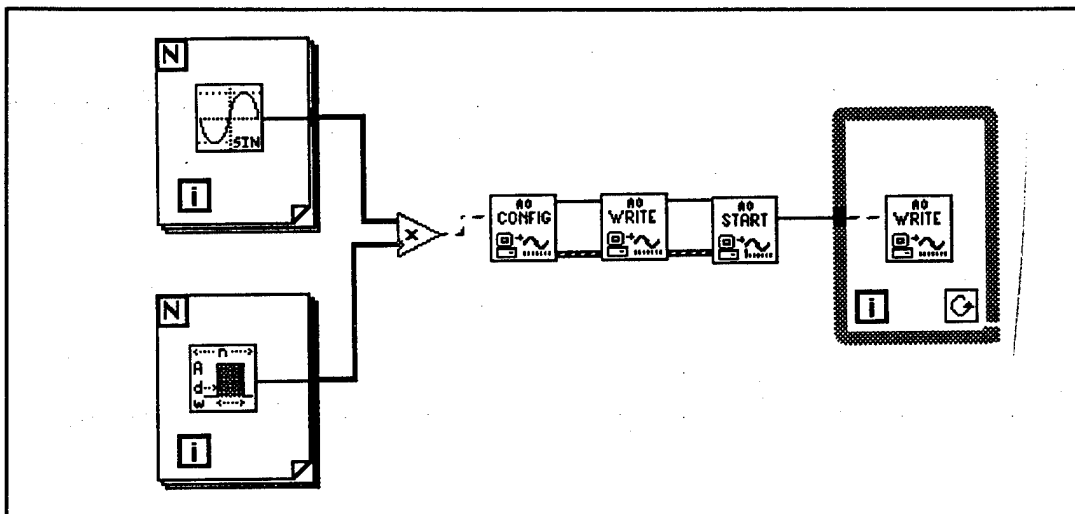


Figure (F.1). Elements of Three Element Function Generator vi.

This basic process is repeated three times, one for each element and then combined into one matrix with each row representing the output of one function generator. This matrix is then sent to an analog output write file which repeats the data inside a "while loop" until it is told to stop. Figure (F.2) is the diagram of the working program.

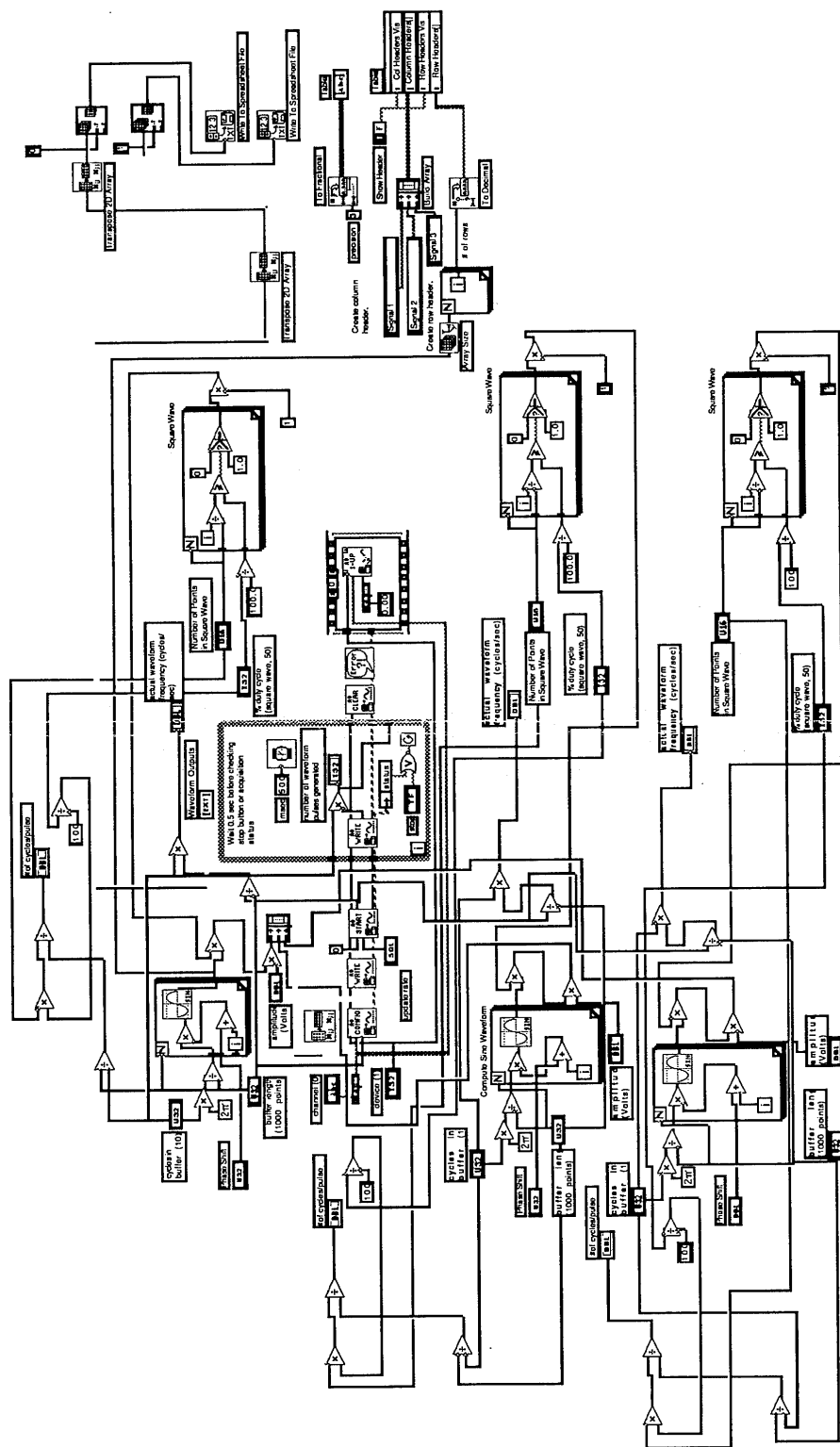


Figure (F.2) Three Element Array Function Generator vi.

## REFERENCES

1. B. Boutros-Ghali, "The Land Mine Crisis, A Humanitarian Disaster," Foreign Affairs, September/October 1994.
2. S. C. Truver, "Exploding the Mine Warfare Myth," Proceedings, October 1994.
3. P. H. Brownell, "Prey Detection by the Sand Scorpion," Scientific America, October 1984.
4. BBN Systems and Technologies Report No. 7677, "Feasibility of Acoustic Landmine Detection. Final Technical Report," May 19, 1992.
5. Kinsler, Coppens, Fry and Sanders, "Fundamentals of Acoustics," John Wiley and Sons, 1982.
6. C. Prada, J. Thomas and M. Fink, "The iterative time reversal process: Analysis of the convergence," J. Acoust. Soc. Am. 97 (1), January 1995.



## INITIAL DISTRIBUTION LIST

1. Defense Technical Information Center.....2  
     Cameron Station  
     Alexandria, Virginia 22304-6145
  
2. Library, Code 013.....2  
     Naval Postgraduate School  
     Monterey, California 93943-5101
  
3. Clyde Scandrett.....1  
     Code MA/Sd  
     Naval Postgraduate School  
     Monterey, California 93943-5101
  
4. Department of Physics.....1  
     Code PH  
     Naval Postgraduate School  
     Monterey, California 93940-5101
  
5. Anthony A. Atchley.....3  
     Code PH/Ay  
     Naval Postgraduate School  
     Monterey, California 93940-5101
  
6. William F. Stewart.....1  
     1095 Spruance Rd.  
     Monterey, California 93940
  
7. Department of Mathematics.....1  
     Code MA  
     Naval Postgraduate School  
     Monterey, California 93943-5101